

Theoretical Study of Transition Metal Dichalcogenides Compound TiS_2 and Their Intercalated Compound $CrTiS_2$ Using Density Functional Theory

<https://doi.org/10.52853/18291171-2021.14.1-37>

Vandana B. Parmar, A. M. Vora

Department of Physics, University School of Sciences, Gujarat University, Navrangpura,
Ahmedabad 380 009, Gujarat, India

E-mail: vandanaparmar3996@gmail.com,
voraam@gmail.com

Received 10 March 2021

Abstract. The Density Functional Theory (DFT) based computational study is carried out for the transition metal dichalcogenides (TMDCs) compound TiS_2 and their intercalated 3d transition metal compound $CrTiS_2$. It is carried through Generalized Gradient Approximation (GGA) through Quantum ESPRESSO environment employing Perdew-Burke-Ernzerhof (PBE) exchange and correlation effect with an ultra-soft pseudopotential. In the present work, the structural optimization and electronic properties like energy band structure, density of states (DOS), partial or projected density of states (PDOS), total density of states (TDOS), Fermi surfaces and charge density are reported. The effect of charge transfer from guest 3d transition metal Cr-atom to self-intercalated compound TiS_2 has been observed. While, the energy band structure of $CrTiS_2$ compound is computed in the non-magnetic state. From the energy band structure of said materials, we conclude that the TiS_2 compound has an indirect narrow band gap though the $CrTiS_2$ compound has an overlapped band structure. The TiS_2 shows a semiconductor or semi-metallic nature while doped compound with guest Cr-atom has a metallic material..

Keywords : Density Functional Theory (DFT); Generalized Gradient Approximation (GGA); Quantum ESPRESSO code; Ultra-soft pseudopotential; Intercalated compound; Transition metal dichalcogenides (TMDCs).

1. Introduction

The study of structural and electronic properties of material gives a basic understanding of the material. In the present work, the intercalated compound Titanium sulphide (TiS_2) has been developed by transition metal general formula TX_2 [1]. The Coulomb interaction has an important in 3d state of transition metal sulphide TiS_2 , because of it will improve the electronic property of TiS_2 . Strong covalent bonding in TiS_2 has existed due to the strong hybridization in Ti (3d-state) and S (3p-state). In TiS_2 , the Ti has a sandwiched layer between two sulphur layers. The outer sulphur and adjacent sulphur layers are weakly connected with the van der Waals forces. It has a very small indirect bandgap or semi-metallic ground state then it has a semiconductor. In very weak van der Waals attraction between interlayer then guest atom can be easily intercalated in pure TiS_2 . Guest atom Cr has intercalated with transition metal TiS_2 , when strong hybridization occurs in $Cr-3d, Ti-3d$ and $S-3p$ states. While, X-ray

Photoemission Spectroscopy (XPS), Angle Resolved Resonant Photoemission Spectroscopy (ARPES), Angle Resolved Inverse Photoemission Spectroscopy (ARIPES) and high field magnetization measurements proved this conclusion by experimentally [2-8]. Similarly from the calculation, d-orbitals of intercalant M-atoms hybridize strongly with s-orbitals. Such that the above calculation says $Cr-S$ bonds stronger than the $Ti-S$ bonds [4]. We concluded that the electronic properties of $CrTiS_2$ have depended on the guest atom like Cr . Sharma *et al.* [9] have reported computational studies of TMDC compounds using density functional theory. Very recently, we have computed electronic and structural properties of various compounds by using first principle approach [10-14].

2. Computational Methodology

The computations in $CrTiS_2$ compound are calculated with the computational code Quantum ESPRESSO [15]. In $CrTiS_2$ the structural optimization and electronic properties such as band structure, density of states, partial density of states, Fermi surfaces and charge density are calculated by using Generalized Gradient Approximation (GGA) [16]. In the present computation, we have used Perdew-Burke-Ernzerhof (PBE) [17] with ultra-soft pseudopotential [18]. To plot the optimization curve and energy band structure, we have utilized gnuplot [19, 20] while for the plots of density of states (DOS), partial or projected density of states (PDOS), total density of states (TDOS), Fermi surfaces and charge density, we have used XCrySDen [21].

3. Results and discussion

In the present section, the spatial attention is drawn about our computationally generated results of said materials.

3.1. Structural optimization

The structural properties are visualized by the lattice constant. The TiS_2 has the CdI_2 -type layer structure. In which, the Ti layer is sandwiched in two sulfur layers. The structure of TiS_2 is shown in Fig. 1(a). In this structure, the unit cell of TiS_2 contains six atoms. In the unit cell position for Ti is a 1a; the two S atoms are positioned in $2d(1/3, 1/3, 0.2501)$ and $(2/3, 1/3, -0.2501)$, respectively. The TiS_2 has a lattice parameters like $a = 3.4285 \text{ \AA}$ and $c = 5.8944 \text{ \AA}$. The structure consists of $S-Ti-S$ sandwiches, separated in the z -direction by the van der Walls gap [9, 14]. Because of very weak van der Walls attraction between the Ti and S layers, the TiS_2 can be easily doped by Cr atom. The lattice position of Cr atom is 1b

(0,0,0.5) in the structure. The structure of $CrTiS_2$ has a hexagonal type with space group $P\bar{3}ml$ [164] as shown in Fig. 2. It has lattice parameters $a = 3.4395 \text{ \AA}$ and $c = 5.9303 \text{ \AA}$. The Brillouin zone (IBZ) for the hexagonal structure as shown in Fig 3. The optimizations of lattice parameters are performed for Titanium Disulphide (TiS_2) and Chromium Titanium Disulphide ($CrTiS_2$). For the relaxation of ground state geometry, three main steps are carried out [15].

1. Convergence of total energy with respect to kinetic energy up to an accuracy of 10^{-4} Ry .
2. Convergence of total energy versus \mathbf{k} – mesh accuracy of 10^{-4} Ry .
3. Optimization of lattice constants to minimize the total energy.

After this, the ratio of lattice parameters (c/a) was optimized to verify the results by using the GGA approach with ultra-soft pseudopotential. In Table 3.1 the computed results of lattice parameters are presented. The optimization curves for TiS_2 and $CrTiS_2$ are shown in Fig. 4 and 5.

Table – 3.1 Calculated lattice parameters for TiS_2 and $CrTiS_2$.

System	Code	Approximation	Lattice Constants (Å)
TiS_2	QE	GGA	$a = 3.4285$ $c/a = 1.7245$
$CrTiS_2$	QE	GGA	$a = 3.4395$ $c/a = 1.7236$

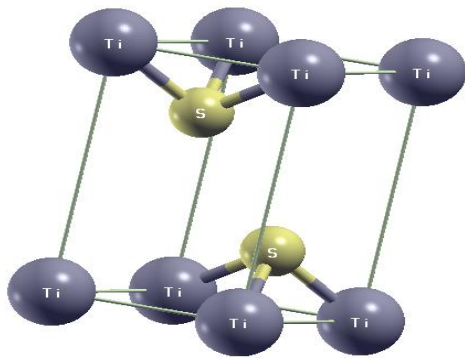


Fig. 1: Crystal structure of TiS_2

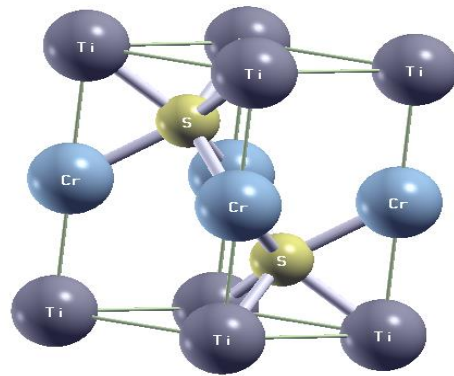
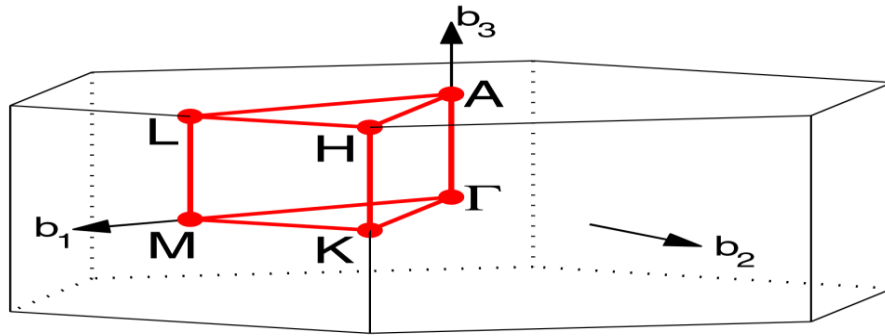


Fig. 2: Crystal Structure of $CrTiS_2$



HEX path: Γ -M-K- Γ -A-L-H-A|L-M|K-H

Fig. 3: Brillouin zone for Hexagonal structure

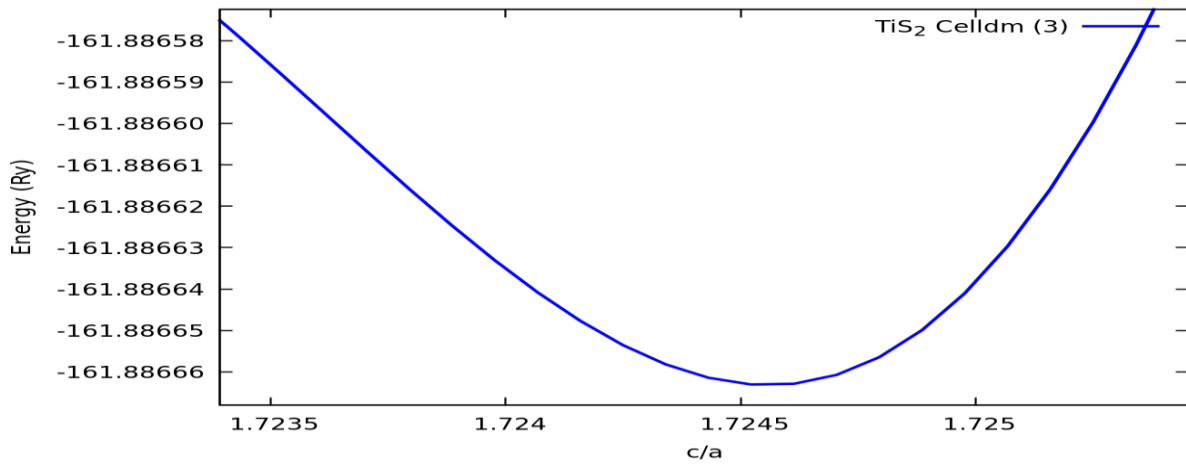


Fig. 4: Optimization curve for TiS₂

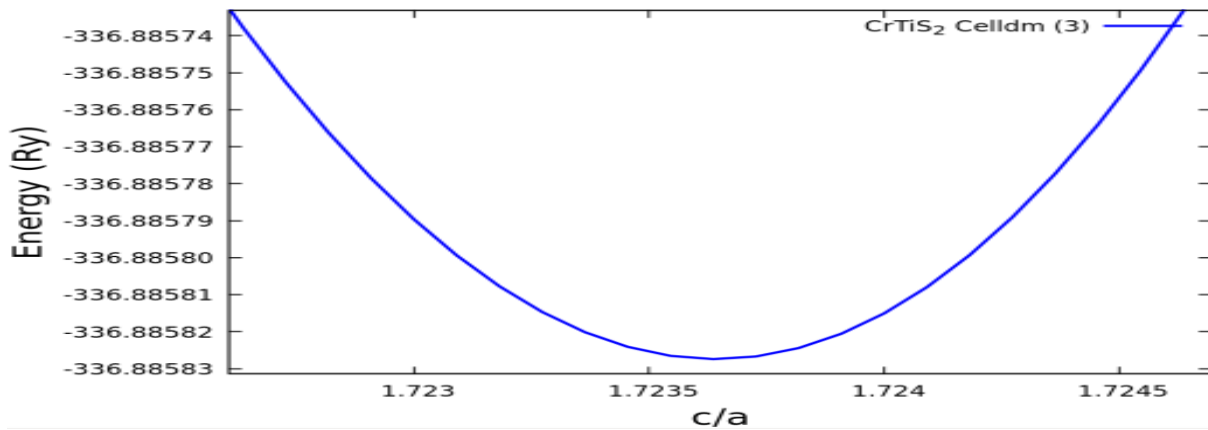


Fig. 5: Optimization curve for CrTiS₂

3.2. Electronic properties

In electronic properties, we have computed the energy band structure, density of states (DOS), total density of states (TDOS), partial or projected density of states (PDOS) and Fermi surfaces with using Density Functional Theory (DFT) with Generalized Gradient Approximation (GGA) [16] through Quantum ESPRESSO code [15].

3.2.1. Band structure

For a crystalline material, a two dimensional representation of energy of the crystal orbital is called band structure. In this work, the band structures of TiS_2 and $CrTiS_2$ compounds are plotted using the gnuplot displayed in Figs. 6 and 7, respectively. In both cases, the \mathbf{k} – points path is considered on the high symmetry points, \mathbf{k} – path. In band structure of both TiS_2 and $CrTiS_2$, \mathbf{k} – point is $\Gamma \rightarrow M \rightarrow K \rightarrow \Gamma \rightarrow A$. For both TiS_2 and $CrTiS_2$ compounds, the kinetic energy cutoff $80Ry$ and charge density cutoff 320 are taken. A \mathbf{k} – mesh of $12 \times 12 \times 12$ is taken on the calculated k-point by the GGA approach.

The energy band structures of TiS_2 shown in Fig. 6 have been plotted in the energy range $-10.0eV$ to $10.0eV$. The \mathbf{k} – path of the band structure is high symmetry directions with the irreducible Brillouin zone (IBZ). In the TiS_2 band structure, it is cleared that TiS_2 has a semiconductor characteristic, as a small indirect bandgap [22, 23]. From Fig. 6, the valance band lines over the Fermi energy but not overlap. Same type of the band structure of $CrTiS_2$ as shown in Fig. 7, it is cleared that the $CrTiS_2$ has a metallic characteristic, as overlapping of band lines near the Fermi region is seen. In $CrTiS_2$, the spin component is added for the computation. Band structures for up spin and down spin are plotted. From Fig. 7 the valance band and the conduction band are overlapped in the energy range $-2.5eV$ to $2.5eV$. Above this, we have concluded that the intercalated compound TiS_2 has a semiconductor characteristic, while the Cr atom has doped than $CrTiS_2$ has a metallic characteristic. In $CrTiS_2$, the band is overlapped maximum at the Fermi level.

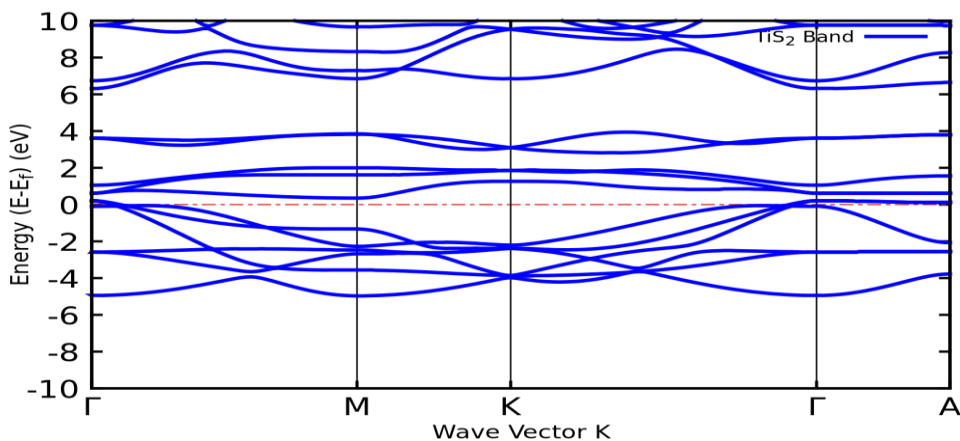


Fig. 5: Electronic band structure of TiS_2

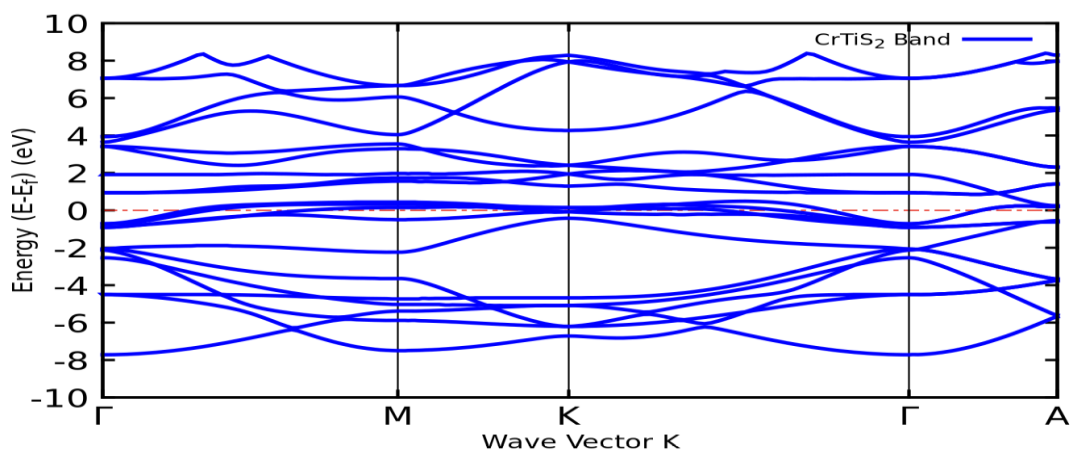


Fig. 6: Electronic band structure of CrTiS_2

In the present work, we observe that the TiS_2 has an indirect bandgap or semi metallic ground state while in CrTiS_2 , the energy bands are overlapped. It is because of doped Cr atom. However, the chromium is a paramagnetic material in nature. Because of it CrTiS_2 has a paramagnetic material. The spin up and spin down in the band structure of CrTiS_2 are having the same nature in the present computation. Hence, only one band structure is shown [4].

3.2.2. Density of States

The number of available energy states, per unit energy per unit volume is the density of states (DOS). From the partial or projected DOS, the contributions from the individual orbitals of different materials, like s, p, d and f, can be checked [22]. We have used the tetrahedral method for integration over the Brillouin zone is used to estimate the DOS. Figs. 8 and 9, show the TDOS and PDOS for TiS_2 . It is plotted in the energy range between -20.0eV to 5.0eV . The electron density of about zero states/eV is observed below the Fermi region at -10.0eV . The density of states of TiS_2 maximum at -5.0eV to 0.0eV . The electron density is of zero states/eV, at the Fermi level. In this, the $S 2p$ -states strongly hybridize with $Ti 3d$ -states. At the Fermi energy level, $Ti 3d$ -states mainly contribute to the conduction band, where the $S 2p$ -states contribute mainly to the valance band [6]. The PDOS of TiS_2 , we have calculated the electron unfilled states, likewise $Ti 3d$ and $S 2p$ -states. In Fig. 9, the PDOS of $Ti 3d$ maximum contributes in the conduction band range 0.0eV to 5.0eV where $S 2p$ maximum contributes in the valance band range -5.0eV to 0.0eV . Since the Cr atom is doped between sulphur layers. In CrTiS_2 , the strong hybridization is seen between $\text{Cr } 3d$ - and $S 3p$ -states, also weak hybridization is observed between $Ti 3d$ - and $S 3p$ -states.

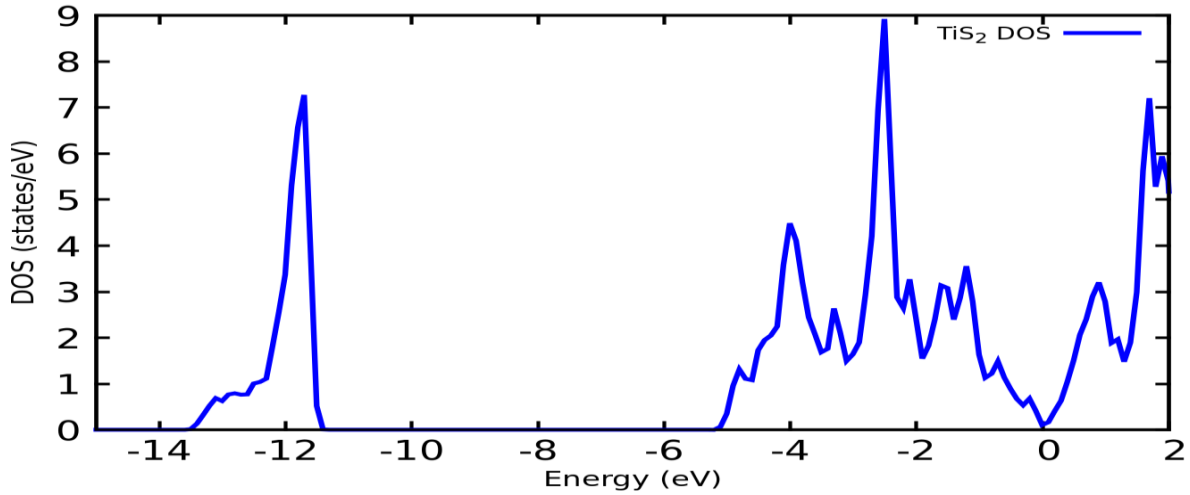


Fig. 8: Total DOS of TiS_2

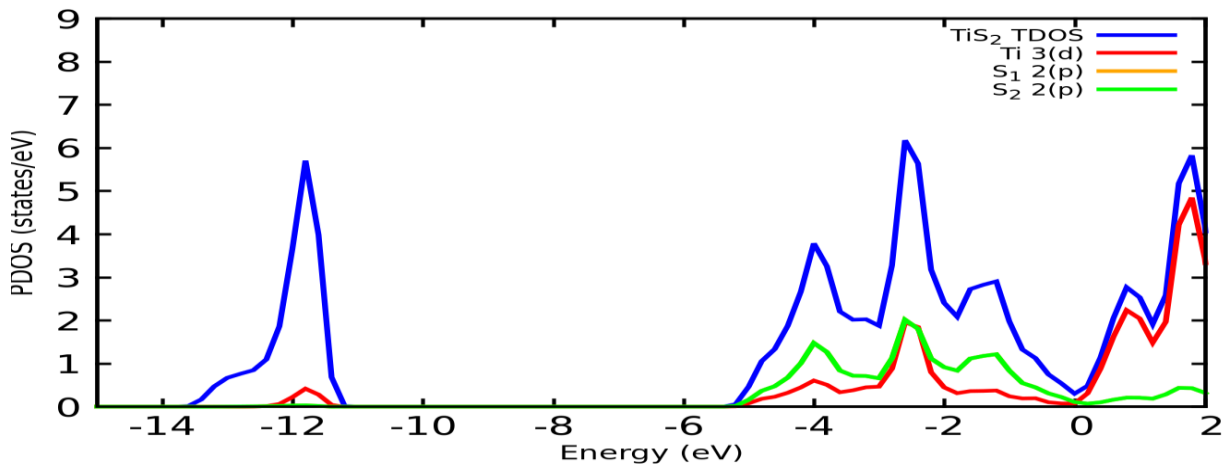


Fig. 9: PDOS for TiS_2

Figs. 10 and 11, show the TDOS and PDOS for $CrTiS_2$ compound. It is plotted in the energy range between $-25.0eV$ to $10.0eV$. In TDOS below the Fermi region, the electron density maximum at 7.5 states/ eV at a point $-5.0eV$ and above the Fermi region the electron density maximum at 6.8 states/ eV at a point $2.0eV$. The density of states at the Fermi region is 8.1 states/ eV . We show that at the Fermi region the density of states is maximum, because of the band overlapping. In PDOS of $CrTiS_2$ is drawn in the states of $Cr 3d$, $Ti 3d$ and $S 2p$ – states. In PDOS, the $Cr 3d$ and $Ti 3d$ – states are mainly contributing to the conduction band, while $S 2p$ – states mainly contributes to the valance band. At the Fermi region, the Cr is maximum. We conclude that the $CrTiS_2$ has a metallic material.

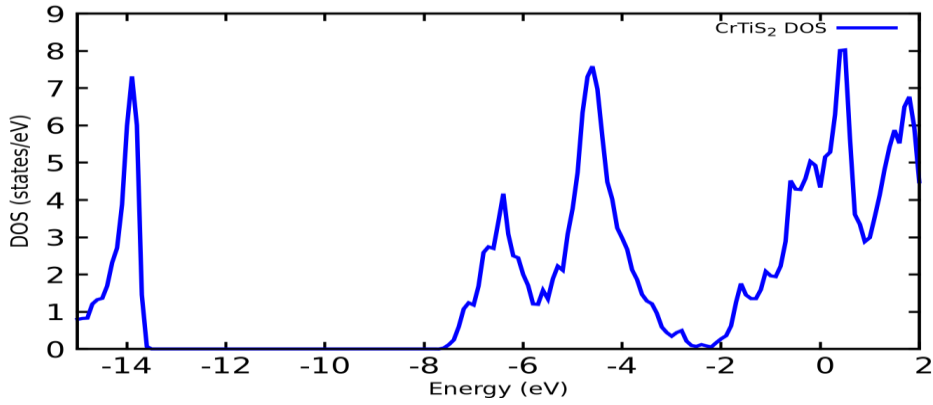


Fig. 10: Total DOS of CrTiS₂

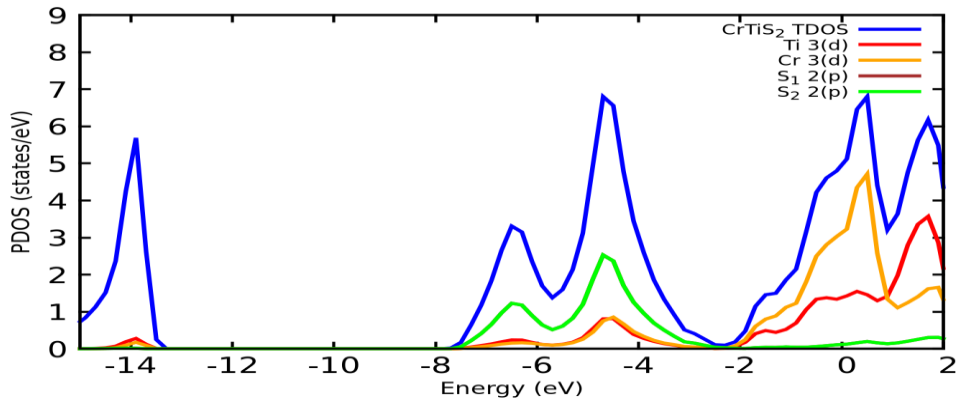


Fig. 11: PDOS for CrTiS₂

3.2.3. The Fermi Surfaces

The Fermi energy is the characteristic energy that distinguishes between the occupied and unoccupied energy levels. It is the concept that helps us to picture the relative occupation of the allowed empty lattice bands geometrically in \mathbf{k} –space [18]. The entire Fermi surface has a constant energy E_F in the momentum space. In other words, it is the surface, where all fermions state with momentum $\mathbf{k} < \mathbf{k}_F$ is occupied and other higher momentum states are unoccupied. Any variation in the unoccupied states around the Fermi surface may lead to the generation of electrical current. Hence, the study of the Fermi surface topology is important to measure the electronic properties of the materials. The software XCrySDen [21] does the visualization of the Fermi surfaces. Figs. 12 (a-d), show the Fermi surfaces for TiS_2 . In the band structure of TiS_2 , there are three bands are crossing the Fermi energy level E_F . The Fermi surface for individual bands passing through the E_F , are shown in Figures 12 (a-c). For merged bands, the Fermi surfaces are displayed in Fig. 12(d). The point-like concentric cylinders are at the zone center (Γ) and the quasi cylinders at the corners of the Brillouin zone in Γ – A direction give the electron contribution. The band in TiS_2 is shifted due to the electron-electron interaction of intercalated atom Cr with both Ti and S atoms.

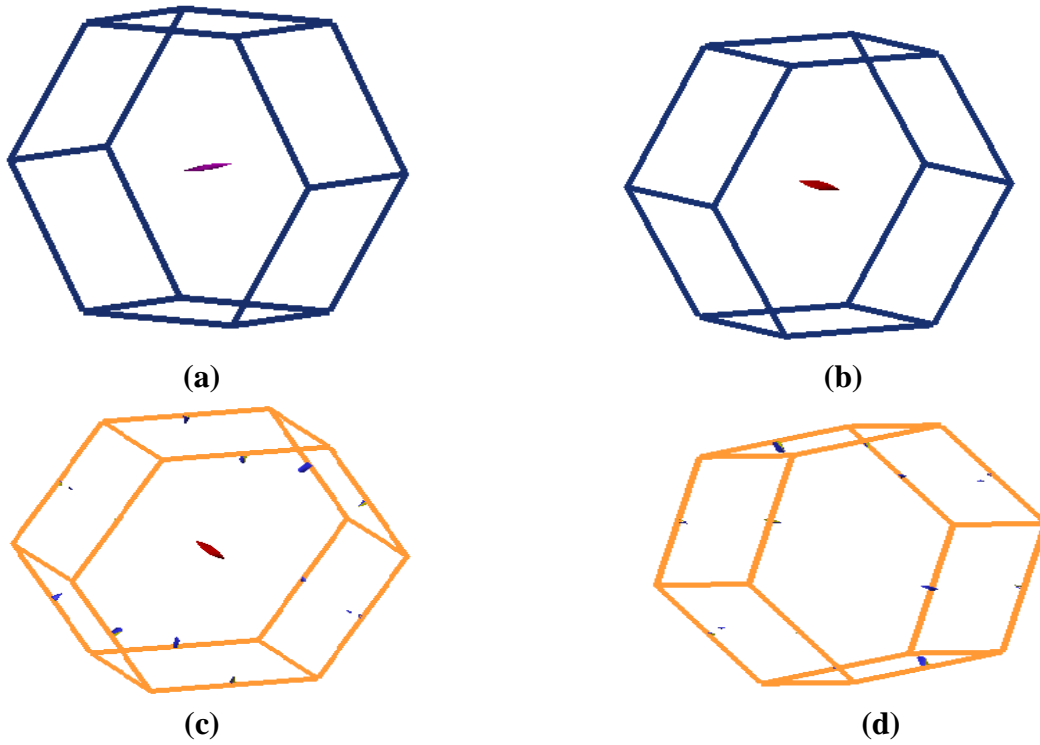


Fig. 12: The Fermi surfaces of TiS_2 for different bands (a) – (c) and for merged band (d).

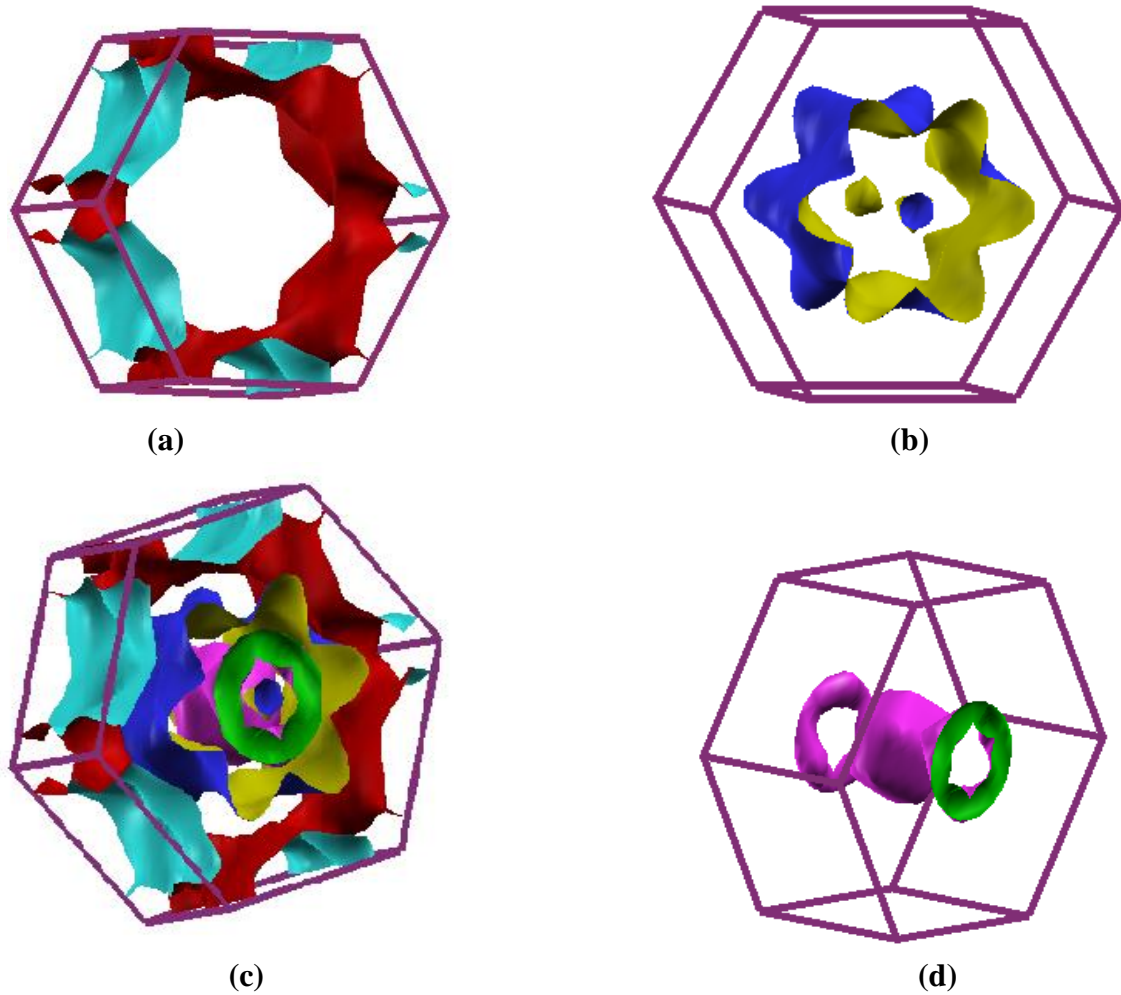


Fig. 13: The Fermi surfaces of CrTiS_2 for different bands (a) – (c) and for merged band (d).

Figs. 13 (a-d), display the Fermi surfaces for $CrTiS_2$ compounds. Here, there are three bands are crossing the Fermi energy level E_F . The Fermi surface for individual bands passing through the E_F , are shown in Figures 13 (a-c). For merged bands, the Fermi surfaces are displayed in Fig. 13(d). The hole-like concentric cylinders are seen at the zone center (Γ) and the quasi cylinders at the corners of the Brillouin zone in $\Gamma - A$ direction give the electron contribution.

3.2.4. Charge density

The electron charge density is the density of electron present at a particular time in the electron cloud of any atom per ion per compound. It can be placed where the probability of electron is found maximum at a particular time. The electron charge distribution of the materials is one of the key quantities in computational materials science as theoretically it determines the ground state energy and practically it is used in many material analyses. In the present work, the charge density is computed through DFT approach. To visualize the nature of charge density in TiS_2 as shown in Fig. 14. It shows that the charge density is shown maximum near the atom at $+1.3672cm^{-2}$ while it is minimum far away the atom at $+0.0690$. In TiS_2 , the charge density near the S atom is minimum while near the Ti atom is maximum. When we doped the guest atom Cr in TiS_2 compound, the charge density increases. However, the charge density of $CrTiS_2$ compound is shown in Fig. 15. It is minimum at $+0.0835cm^{-2}$ while maximum near the atom at $+2.7817cm^{-2}$.

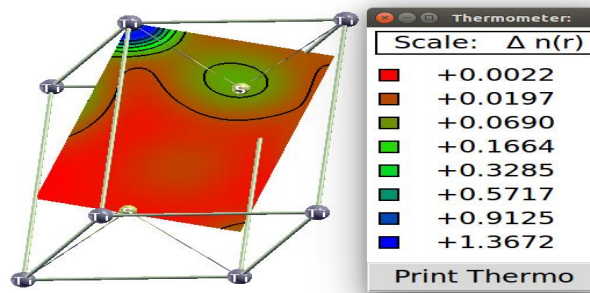


Fig. 14. Charge density of TiS_2 .

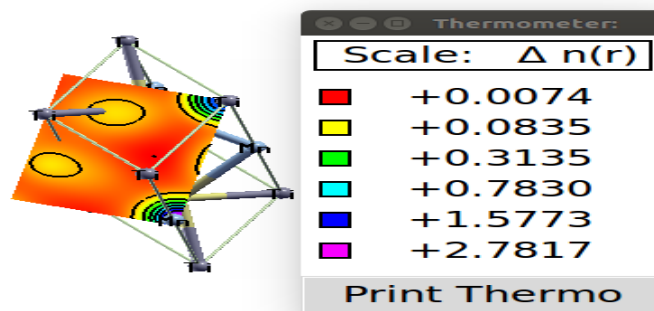


Fig. 15. Charge density of $CrTiS_2$.

4. Conclusions

In this work, we conclude that, the structural analysis like lattice constants and electronic properties visualized electronic band structure, total and projected density of states (TDOS and PDOS), Fermi surfaces of intercalant compound and charge density of TiS_2 and $CrTiS_2$ both compounds are computed by using GGA, including the exchange correlation effects with the functional proposed by PBE [17] through Quantum ESPRESSO [15] code. In structural optimization, Cr atom is placed between TiS_2 interlayer. While, in electronic band structure, the TiS_2 has a small indirect band gap or semi-metallic band structure while when doping with Cr atom then change the band structure. The $CrTiS_2$ have overlapping conduction band and valance band and possesses metallic structure. For TDOS and PDOS in TiS_2 and $CrTiS_2$, at Fermi energy level, $Cr 3d$ and $Ti 3d$ states are mainly contributed in the conduction band, while $S 2p$ -states contribute mainly to the valance band. The TDOS and PDOS of TiS_2 is studied nearer to zero at the Fermi energy level while for $CrTiS_2$, it is maximum at 3.0 states/eV near Fermi energy region. The Fermi surfaces corresponding to the energy bands intersecting the Fermi level shows the electronic contribution in the band structure of $CrTiS_2$. In TiS_2 , such electronic contribution is shown minimum because of the bands are not overlapping in Fermi region. The electron contribution maximum in $CrTiS_2$ at point M and K . the charge density can be increased while guest atom Cr intercalated in TiS_2 compound.

Acknowledgment

We sincerely acknowledged the computational facility developed under DST-FIST programme from DST, Government of India, New Delhi, India and financial assistance under DRS-SAP-II from UGC, New Delhi, India.

References

- [1] K. Motizuki, N. Suzuki, Phys. New Mater. **27** (1994) 106.
- [2] N. Suzuki, Y. Yamasaki, K. Motizuki, J. de Physiq. Solid State Phys. **C8** (1998) 201.
- [3] R. H. Friend, A. D. Yoffe, Adv. Phys. **36** (1987) 1-94.
- [4] J. A. Wilson, A. D. Yoffe, Adv. Phys. **18** (1969) 193.
- [5] T. Yamasaki, N. Suzuki, K. Motizuki, J. Phys. C: Solid State Phys. **20** (1987) 395.
- [6] T. Matssushita, S. Suga, A. Kimuta, Phys. Rev. **B60** (1999) 1678.
- [7] Y. Ueda, H. Negishi, M. Koyana, M. Inoue, Solid State Comm. **57** (1986) 839.
- [8] Y-S. Kim, J. Li, I. Tanaka, Y. Koyama, H. Adachi, Mat. Trans. Jim. **8** (2000) 1517.
- [9] Y. Sharma, S. Shukla, S. Dwivedi, R. Sharma, Adv. Mater. Lett. **6** (2015) 294.
- [10] V. B. Zala, A. M. Vora and P. N. Gajjar, AIP Conference Proc. **2100** (2019) 020027.
- [11] H. S. Patel, V. A. Dabhi and A. M. Vora, in: D. Singh, S. Das, A. Materny (Eds.), Advances in Spectroscopy-Molecules to Materials, Springer Proc. Phys. **236** (2019) 389.
- [12] V. A. Dabhi, H. S. Patel and A. M. Vora, AIP Conf. Proc, **2224** (2020) 030003.
- [13] H. S. Patel, V. A. Dabhi and A. M. Vora, AIP Conf. Proc, **2224** (2020) 030006(1).
- [14] V. B. Parmar and A. M. Vora, East Eur. J. Phys. **1** (2021) 93.

- [15] P. Giannozzi, S. Baroni, N. Bonini, M. Calandra, R. Car, C. Cavazzoni, D. Ceresoli, G. Chiarotti, M. Cococcioni, I. Dabo, A. Dal Corso, J. Phys. Condens. Matter **21** (2009) 395502.
- [16] J. P. Perdew, J. Chevary, S. Vosko, K. Jackson, M. Perderson, D. Singh, C. Fiolhais, Phys. Rev. B **48** (1993) 4978.
- [17] J. P. Perdew, K. Burke, M. Ernzerhof, Phys. Rev. Lett. **77** (1996) 3865.
- [18] <http://www.quantum-espresso.org/pseudopotential>.
- [19] P. K. Janert. Gnuplot in action: understanding data with graphs.
- [20] P. K. Janert, J. Cheminform. **3** (2011) 1.
- [21] A. Kokaji, XcrySDen- -a new program for displaying crystalline structures and electron densities, **17**(3-4), 176-9, 215-6.
- [22] C. M. Fang, R. A. de Groot, C. Hass, Phys. Rev. B **56** (1997) 4455.
- [23] Q. Yan-Bin, Z. Guo-Hua, LI Di, W. Jiang-Long, Q. Xiao-Ying, Z. Chi. Zhi, Phys. Lett. **24** (2007) 1050.